Earthquakes and Structures, *Vol. 22, No. 5 (2022) 503-515*
https://doi.org/10.12989/eas.2022.22.5.503

Seismic fragility curves for a concrete bridge using structural health monitoring and digital twins

Norberto Rojas-Mercedes[1], Kalil Erazo[*1,2] and Luigi Di Sarno[3,4]

[1]*School of Engineering, Instituto Tecnológico de Santo Domingo (INTEC), Santo Domingo, Dominican Republic*
[2]*Department of Civil and Environmental Engineering, Rice University, Houston, Texas, USA*
[3]*Department of Civil Engineering and Industrial Design, School of Engineering, University of Liverpool, Liverpool, United Kingdom*
[4]*Department of Engineering, University of Sannio, Benevento, Italy*

(Received November 17, 2021, Revised March 19, 2022, Accepted April 14, 2022)

Abstract. This paper presents the development of seismic fragility curves for a precast reinforced concrete bridge instrumented with a structural health monitoring (SHM) system. The bridge is located near an active seismic fault in the Dominican Republic (DR) and provides the only access to several local communities in the aftermath of a potential damaging earthquake; moreover, the sample bridge was designed with outdated building codes and uses structural detailing not adequate for structures in seismic regions. The bridge was instrumented with an SHM system to extract information about its state of structural integrity and estimate its seismic performance. The data obtained from the SHM system is integrated with structural models to develop a set of fragility curves to be used as a quantitative measure of the expected damage; the fragility curves provide an estimate of the probability that the structure will exceed different damage limit states as a function of an earthquake intensity measure. To obtain the fragility curves a digital twin of the bridge is developed combining a computational finite element model and the information extracted from the SHM system. The digital twin is used as a response prediction tool that minimizes modeling uncertainty, significantly improving the predicting capability of the model and the accuracy of the fragility curves. The digital twin was used to perform a nonlinear incremental dynamic analysis (IDA) with selected ground motions that are consistent with the seismic fault and site characteristics. The fragility curves show that for the maximum expected acceleration (with a 2% probability of exceedance in 50 years) the structure has a 62% probability of undergoing extensive damage. This is the first study presenting fragility curves for civil infrastructure in the DR and the proposed methodology can be extended to other structures to support disaster mitigation and post-disaster decision-making strategies.

Keywords: civil infrastructure; digital twins; earthquake engineering; fragility curves; structural health monitoring

1. Introduction

The Hispaniola Island is located in the Caribbean and includes the Republic of Haiti and the Dominican Republic (DR). The island is considered a high seismic hazard region due to the convergence of the North American and Caribbean plates; there are more than 10 active seismic faults with high strain rates throughout the island (see Fig. 1). The damage potential of the Hispaniola's active seismic faults was demonstrated after the 2010 Haiti earthquake, considered one of the most devastating natural disasters in recent history (Neris *et al*. 2010). The 2010 Haiti earthquake was caused by a rupture at the Enriquillo fault (labeled "(11) EPGEZ" in Fig. 1) with a death toll estimated at 300,000 and an economic loss estimated at nearly US$14 billion, exceeding the gross domestic product of the country. The disaster demonstrated the consequences of a weak physical infrastructure, as well as weaknesses of government institutions (DesRoches *et al*. 2011). More recently, on August 14, 2021, another major earthquake of 7.2 magnitude was caused by a rupture at the same fault, also resulting in major life and economic losses.

The motion of the Caribbean plates has been the focus of research studies aimed at estimating the strain accumulation and fault slip rates (which can be correlated to energy accumulation and potential earthquake magnitude) using GPS geodetic data for several years prior to the occurrence of the 2010 Haiti earthquake (Calais *et al*. 1992, Calais *et al*. 2002). Based on these studies, Calais *et al*. (2002) concluded that the Enriquillo and Septentrional faults (the latter labeled "(3) SFZ" in Fig. 1) have the potential to generate major destructive earthquakes. Recent research supports that the Septentrional fault is likely in the late phase of its rupture cycle with a characteristic earthquake of 7.8 magnitude. The Septentrional fault is the main source of seismic hazard in the DR and has been the focus of research to estimate the maximum earthquake it can potentially generate and its effects on civil infrastructure (Mann *et al*. 1994, Calais *et al*. 2002, Frankel *et al*. 2011, Erazo 2019, 2020).

In addition to the exposure to earthquakes, the exposure of the DR to other extreme natural hazards has been evaluated and compared with 32 other countries in the Latin America and Caribbean region by the Disaster Risk Management Knowledge Center of the European Commission (INFORM, 2019). Based on this assessment the country obtained a score of 8.4/10 for physical exposure

*Corresponding author, Ph.D.
E-mail: kalil.erazo@intec.edu.do

ISSN: 2092-7614 (Print), 2092-7622 (Online)

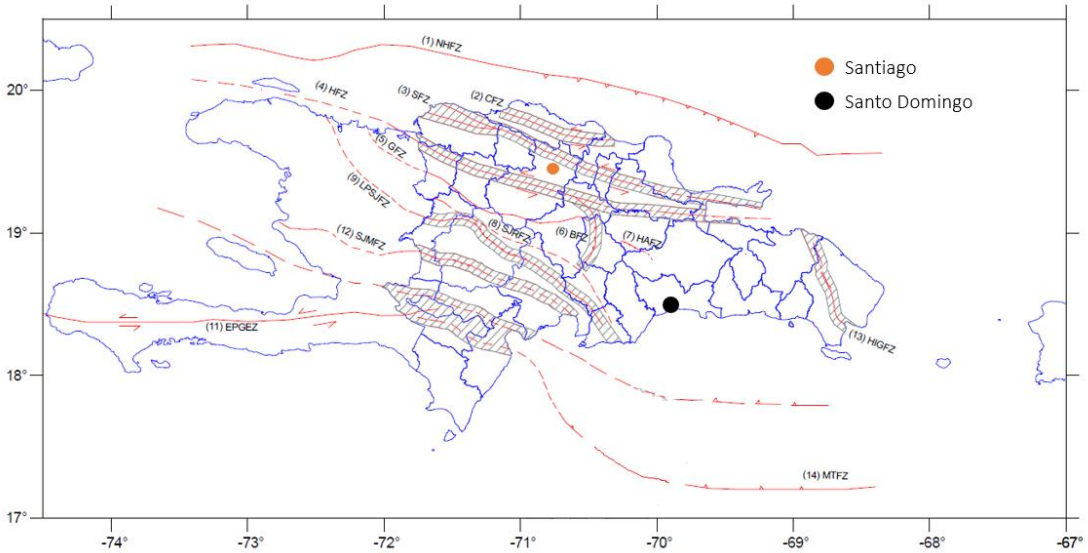

Fig. 1 Seismic faults in The Hispaniola (Ministerio de Obras Públicas y Comunicaciones 2011). Continuous and dashed lines indicate the location of the main active seismic faults

to earthquakes (place 7/33), a score of 8.7/10 for physical exposure to tropical cyclones (place 3/33), and an overall score of 7.1/10, which places the DR as one of the countries with highest natural disaster risk in the region. Other similar studies have reached a similar conclusion (GFDR 2007).

Due to the high seismicity and energy accumulation in the seismic faults in the northern region of the DR, it is of interest to assess the state of structural integrity of civil infrastructure in order to retrofit vulnerable structures, prioritizing the use of the limited economic resources available to structures that serve as the essential lifeline to multiple communities. This issue is further exacerbated by the fact that most of the civil infrastructure in the country were designed using outdated building codes and regulations with design loads significantly smaller than those determined based on recent seismic hazard assessments for the region. Bridges, which are key components for transportation and communication, have a preponderant role in the development of a country and the mitigation efforts of first responders in the aftermath of damaging earthquakes. The important role of bridges in post-disaster rescue operations in remote regions of the DR has been evident after the multiple collapses registered during past events. Fig. 2 shows the collapse of bridges during two recent storms, leaving the affected communities isolated and without access to food and health care for more than a month. During the first storm (Noel) 25 bridges collapsed, while during the second storm 42 bridges collapsed.

Fig. 2 Recent precast bridges collapse in the DR (Rodríguez and López 2007, Batista 2017)

The collapse of bridges has shown to be a major constraint for the emergency response system of the DR, especially due to the lack of redundancy with communities that depend on a single access to receive assistance from first responders after a disaster. Bridges in the northern region of the DR are of special interest due to their closeness to active seismic faults with significant energy accumulation and the potential to generate strong earthquakes. A significant portion of these bridges are short-span bridges consisting of single-span or multiple-span precast post-tensioned reinforced concrete girders; this is also the case for other countries in the Caribbean region such as Haiti and Puerto Rico, and thus the results presented herein can be extended for earthquake damage assessment in these countries. For this reason it is of interest to assess the vulnerability and estimate the performance of this class of bridges (Zhang and Hu 2005, Rossetto and Elnashai 2005).

A useful tool to quantitatively predict the seismic performance of structures are fragility curves. Fragility curves provide an estimate of the probability of potential damage limit states as a function of a measure of ground motion intensity, such as peak ground acceleration or spectral acceleration (Nielson and DesRoches 2007, Baker 2015, Naderpour and Vakili 2019). To develop fragility curves analytical methods based on using a computational model to predict structural response parameters are typically employed. The development of fragility curves requires the non-trivial task of defining the nature of the expected strong motion and ground motion characteristics, either recorded from past earthquakes or generated synthetically using a stochastic process model (Bakhshinezhad and Mohebbi 2019, Karimzadeh *et al*. 2020 Surana 2020). Moreover, the computational models can incorporate modeling uncertainty for parameters or properties of the ground motion and/or the structure, such as material properties, section properties, boundary conditions, among others (Padgett and DesRoches 2008, Elnashai and Di Sarno 2008, Tavares *et al*. 2012, Razzaghi *et al*. 2018).

An important current limitation and source of errors when formulating and applying fragility curves to predict structural performance is modeling uncertainty, that is, errors in predicting structural response and damage parameters due to inherent limitations of the structural models employed; these errors are of both parametric and non-parametric nature. Although modeling uncertainty can be partially accounted for by using a probabilistic model (such as treating material properties as random variables), parameters that best fit a model of a structure vary significantly even for structures with similar physical characteristics. A significant reduction in modeling uncertainty and improvement in the accuracy of the fragility curves is achieved by employing a digital twin that, in addition to a physics-based computational model, incorporates measured data directly obtained from the structure of interest using a structural health monitoring (SHM) system. A digital twin consists on a cyber-physical system that combines a computational model with measured data, resulting on a tool with increased predicting capabilities. In this context SHM is employed to extract the vibration characteristics of a structure from response measurements and subsequently incorporating this information in the structural performance assessment (Nagarajaiah and Erazo 2016, Erazo *et al*. 2019a, Erazo *et al*. 2019b). Depending on the type and characteristics of the available data, both linear and nonlinear characteristics of the model can be incorporated in the analysis. Probabilistic approaches and SHM can be combined into a holistic comprehensive analysis to develop a probabilistic digital twin that is conditional on the measured data.

In the context of bridges, fragility curves have been developed in different countries and for different types of structures (Wu *et al*. 2012, Feng *et al*. 2018, Kehila *et al*. 2018, Martin *et al*. 2019, Yon 2020, Zhao *et al*. 2021). Nielson (2005) generated fragility curves to assess the seismic vulnerability of the most common types of bridges in the central and southeast regions of the United States using analytical methods. Fragility curves were generated for four levels of damage (slight, moderate, extensive and complete). The fragility curves developed showed that the most vulnerable bridge classes were those that use steel beams. Moschonas *et al*. (2009) evaluated the seismic vulnerability of typical bridges located on modern highways in Greece using fragility curves. A total of 11 different classes of bridges were identified according to their geometric and structural characteristics. The fragility curves obtained were calibrated with empirical curves based on damage data from the United States and Japan (Yamaguchi and Yamazaki 2000, Mieses *et al*. 2007). Avşar *et al*. (2011) conducted the first study of vulnerability of bridges in Turkey using fragility curves for typical road bridges built after 1990. From a total of 52 bridges evaluated, 4 typical classes were identified based on their structural characteristics. The structural model was subjected to 25 earthquakes recorded in Turkey and the response of the structure was measured in terms of the maximum ground velocity (PGV), maximum acceleration (PGA) and acceleration intensity spectrum (ASI). The fragility curves were developed for three limit states, namely serviceability, damage control and collapse prevention. Gómez and Soria (2013) used fragility curves to study the seismic vulnerability of three bridges located in the Pacific of Mexico. For each selected structure a computational numerical model was developed considering non-linear effects on the columns. Some of the models were calibrated by means of environmental vibration measurements and damage probability matrices were built to serve as the basis for the generation of fragility curves and the identification of the most vulnerable elements of each analyzed structure.

De Risi *et al*. (2017) evaluated the seismic behavior of existing bridges originally designed only for gravitational loads typical of earthquake-prone regions in southern Europe. As a case study, a bridge located in the Northeast of Italy built in the 1970s was selected. The seismic response of the bridge was evaluated through advanced nonlinear dynamic analyses using earthquake records compatible with the location of the bridge according to the seismic hazard determined by the Italian Institute of Geography and Volcanology (INGV). The far-field and near-field effects were considered using two sets of 30 earthquakes each. To derive the fragility curves, the peak ground acceleration (PGA) was used as a measure of intensity and three parameters of structural. It was observed that the near-field records imposed higher and more variable demands on the fragile components of the bridge than the far-field records. However, fragility curves related to far-field records exhibited greater probabilities of failure than those related to nearby records.

Wilches *et al*. (2019) evaluated the seismic risk of a typical bridge representative of the roads in Chile using fragility curves with the objective of evaluating the effectiveness of the design code improvements implemented after the 2012 8.8 magnitude earthquake. For the evaluation, statistical analyses were performed using a database of bridges provided by the Ministry of Public Works of Chile (MOP), from which a representative structure of the bridges in the country was selected. To obtain the fragility curves a simplified 2D model was

assessed through dynamic nonlinear analysis using the accelerations of 117 horizontal accelerograms. Three damage states were defined conforming to those corresponding to the damage observed after the 2012 earthquake. From the generated curves, the authors concluded that the seismic behavior of the bridges in Chile depends mainly on the type of soil and not on the seismic zone in with are located. In turn, it was observed that the improvements implemented in the code resulted in a significant increase in the security of these structures. More recently, the use of machine learning algorithms has been proposed as a tool to develop fragility curves (Mangalathu and Jeon 2019, Mangalathu *et al*. 2019). The accuracy and effectiveness of the proposed methodology was demonstrated in the context of a class of bridges designed for California considering modeling uncertainty.

This paper presents the development of fragility curves for a precast post-tensioned reinforced concrete girder bridge located close to the Septentrional fault in the DR. To reduce modeling uncertainty a SHM system was installed on the bridge to provide a more accurate assessment of its state of structural integrity, and to predict its performance and state of damage after a potential earthquake. The adopted methodology can be summarized as follows:

- Identify the typical bridges in the DR and their structural and geometric characteristics
- Select a bridge of the largest class of typical bridges for a case study
- Instrument the bridge with an SHM system
- Determine the dynamic characteristics from SHM data
- Develop digital twins by combining computational structural models and SHM data
- Generate the fragility curves using the digital twins

As mentioned before, fragility curves need to be developed for specific locations given their sensitivity to the type of structural system, material properties, local soil characteristics, seismic faults characteristics near the site, among other parameters that strongly depend on the site location and local design and construction methods. In the case of the DR, fragility curves have not been developed for any type of structure. The motivation for this work is to serve as a starting point to build a database with which the local government and other stakeholders can base their decisions on the process of inspection, maintenance and/or rehabilitation of structures for disaster mitigation.

2. Fragility curves

Fragility curves are probabilistic models that describe the likelihood of a structure or structural component exceeding various damage limit states. More specifically, the curves define the probability that a structural demand exceeds a certain threshold, conditional on a parameter of the ground motion which typically is selected as the peak ground acceleration (PGA) (Shinozuka *et al*. 2000). Based on previous research a lognormal distribution is generally adopted for seismic demands or damage limit states, and thus the fragility of a component or structure is defined as

Table 1 Strain demand thresholds for different concrete crushing damage limit states

Damage state			
Slight	Moderate	Severe	Complete
0.001	0.002	0.003	0.0044

Fig. 3 El Cacique Bridge; bridge deck and access ramp

$$p[D|PGA] = \Phi\left(\frac{\ln(PGA) - \mu_{ln}}{\sigma_{ln}}\right) \quad (1)$$

where Φ is the standard normal cumulative distribution, D is an event related to a damage limit state; μ_{ln} and σ_{ln} are model parameters of the probabilistic model obtained from a regression analysis or model fitting.

The damage limit states used in this study are defined as follows:

- **No Damage**: No evident significant physical changes to the structure.
- **Slight (minor) damage**: Minor cracking and/or spalling. No jeopardizing of structural safety or performance.
- **Moderate damage**: Moderate flexure/shear cracks; moderate abutment movement. Structural performance affected but the structure's functionality remains uninterrupted; repairs/intervention needed.
- **Severe (extensive) damage**: Major cracking and degradation without collapse; major abutment movements. Structural safety jeopardized and the structure's functionality is interrupted; the structure is likely in an irreparable state.
- **Complete damage**: Partial, total or imminent collapse; loss of ground supports. Decommission of the structure (or a significant portion) required.

The definition of the different damage limit states are based on a measure of the response of the structure, such as relative displacements, plastic rotations, ductility, demand-to-capacity ratios of the structural elements, deformations, among others. In the case of precast reinforced concrete girders whose behavior is dominated by bending, and with a ductility level such that failure is due to concrete crushing, the maximum unit strain deformation in the concrete can be selected as the demand parameter to assess the structural

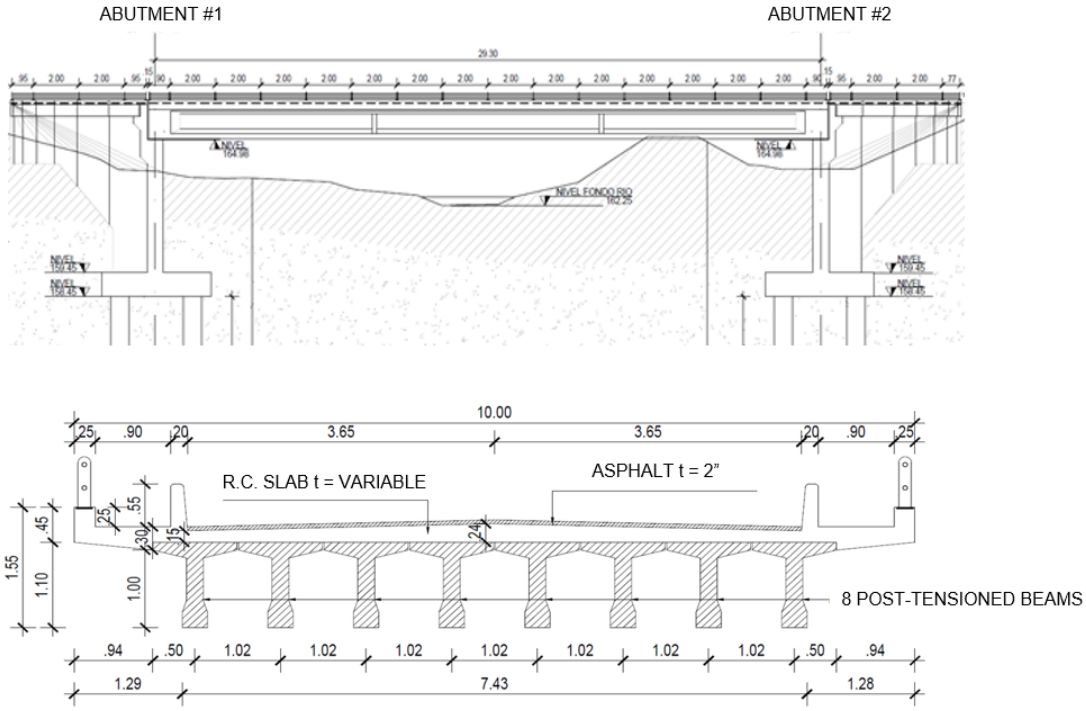

Fig. 4 El Cacique Bridge schematic drawings showing the main structure and precast girders

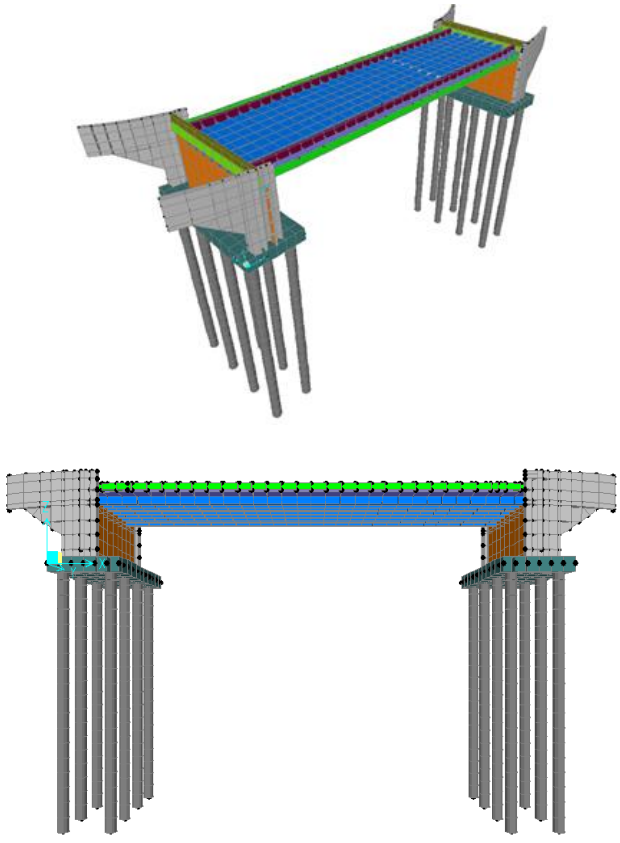

Fig. 5 3D views of the bridge computational model

damage. The limit states for this parameter are defined in Table 1. The values were adapted from the work of Calvi (1999) taking into consideration the local characteristics of the materials used to build civil infrastructure in the DR.

3. Case study: Structure description

The most common type of bridge in the built environment of the DR consists of precast post-tensioned reinforced concrete girders, supported on abutments or piers. In addition to being designed with outdated codes and regulations, a significant portion of these bridges are located in the northern region of the country, a zone of high seismic hazard. A typical bridge of this class is selected as a case study to develop a set of fragility curves for earthquake performance assessment. The bridge is shown in Fig. 3.

The selected bridge is located in the community El Cacique (Moca) at a distance of approximately 5 miles from the Septentrional fault; this is an active fault with a 7.8-magnitude characteristic earthquake. The bridge has a single 29.6m span. The superstructure consists of a reinforced concrete deck of variable thickness from 0.15m at the ends to 0.24m at midspan. The deck is supported by eight AASHTO Type IV post-tensioned beams, spaced 1.02 m from center to center. The abutments are supported by a deep foundation, consisting of eight reinforced concrete piles poured in situ, each of 0.80m diameter and 18m deep. Fig. 4 shows a schematic drawing of the bridge.

4. Computational model

In order to assess the seismic structural vulnerability of the bridge using fragility curves, a finite element model was developed considering the structural specifications and detailing of the elements described in the previous section; the geometry used to develop the model was based on the structural drawings used for construction. The computational model was developed in the commercial

finite element software CSIBridge (Computers and Structures 2020). The computational model (shown in Fig. 5) accounts for the abutments flexibility and soil-foundation-structure interaction using zero-length springs. For the bridge under study the backfill is a gabion rock structure with a significant gap between the backfill and the abutments to avoid interaction between the backfill and the bridge; for this reason no backfill compression is considered in the model. The analyses performed confirmed that the gap is sufficient to prevent contact. Based on the geotechnical studies performed at the site the abutments pile springs stiffness was selected as 0.25 kN/mm; the stiffness is assumed to be provided only by the piles and modeled by zero-length springs.

The bridge deck and abutments were modeled using shell-thin elements, the girders were modeled as nonlinear layered finite elements, and the piles were modeled as frame elements. The model accounts for the restraining effect of the soil on the piles using elastic springs with properties obtained from the geotechnical study performed for the site. The beams were modeled as nonlinear shell layered elements with the rebar layer defined according to the amount of reinforcement provided using an equivalent "smeared" thickness; in these elements the section is divided into several layers to which a stress-strain relationship is assigned according to the material properties defined on the structural drawings.

The dead load consists of the weight of the structural components and an additional superimposed dead load of 1.0 kN/m^2 to account for asphalt and non-structural components, and 1.40 kN/m^2 for the sidewalks; the loads were defined based on current DR building code specifications. The live load was defined according to the AASHTO standard considering the HS-44 truck for analysis (AASHTO 2012).

Fragility curves are employed herein for seismic performance assessment based on the damage limit states defined in previous sections. To estimate the demand of the bridge due to seismic effects a nonlinear time-history response analysis is performed based on recorded ground motions that resemble the characteristics near the site. The computer program REXEL (Iervolino *et al*. 2010) was used to select a set of 11 acceleration records compatible with the design response spectrum for the bridge site. The records were scaled so that the peak acceleration (PGA) was 0.05, 0.15, 0.25, 0.35, 0.45, 0.55, 0.65, 0.75, 0.85 0.95 and 1.05, which implies that the structure was analyzed 11 times for each accelerogram, resulting on a total of 121 analyzes.

5. Structural health monitoring and digital twin

In order to improve the state of knowledge of the bridge and reduce modeling uncertainty structural health monitoring (SHM) was used. The objective of SHM is to extract information about the structure of interest using sensors that measure structural response characteristics. The premise is that SHM measured data is sensitive to physical changes in the structure and can thus be used as an effective tool in the assessment of the state of integrity of the structure. In the context of this work, acceleration response measurements are used to estimate the vibration characteristics of the bridge (vibration frequencies, modes, and damping ratios), and to develop a digital twin that is consistent with the estimated properties. The use of a digital twin that combines a physics-based computational model with SHM data results in a prediction of structural demands with reduced uncertainty, minimizing modeling errors and providing estimates that are in agreement with the measured characteristics of the bridge.

Fig. 6 Bridge instrumentation consisting of 10 wireless triaxial accelerometers

The instrumentation consisted of 10 triaxial wireless accelerometers (shown in Fig. 6) located at different spatial locations throughout the bridge. The sensors synchronously measured the acceleration response at a 32Hz frequency. The locations of the sensors are depicted in Fig. 7. As can be seen the instrumentation is such that the measurements can capture both flexure and torsion vibration modes.

Two types of tests were considered during the SHM program, namely, ambient vibrations and free vibrations induced by an impact load. To excite the bridge for the free vibration case an impact source in the form of a truck of known weight was used. A movable bump was placed at different locations on the bridge to generate an impact inducing a free vibration response. Fig. 8 shows the two cases considered in the experiment with the bump located at the mid-span, and a case with the bump located at a quarter of the bridge span measured from the abutment.

A sample of the vibration response measurements for both free and ambient vibrations are shown in Fig. 9. The measurements consist of the vertical accelerations at mid-span.

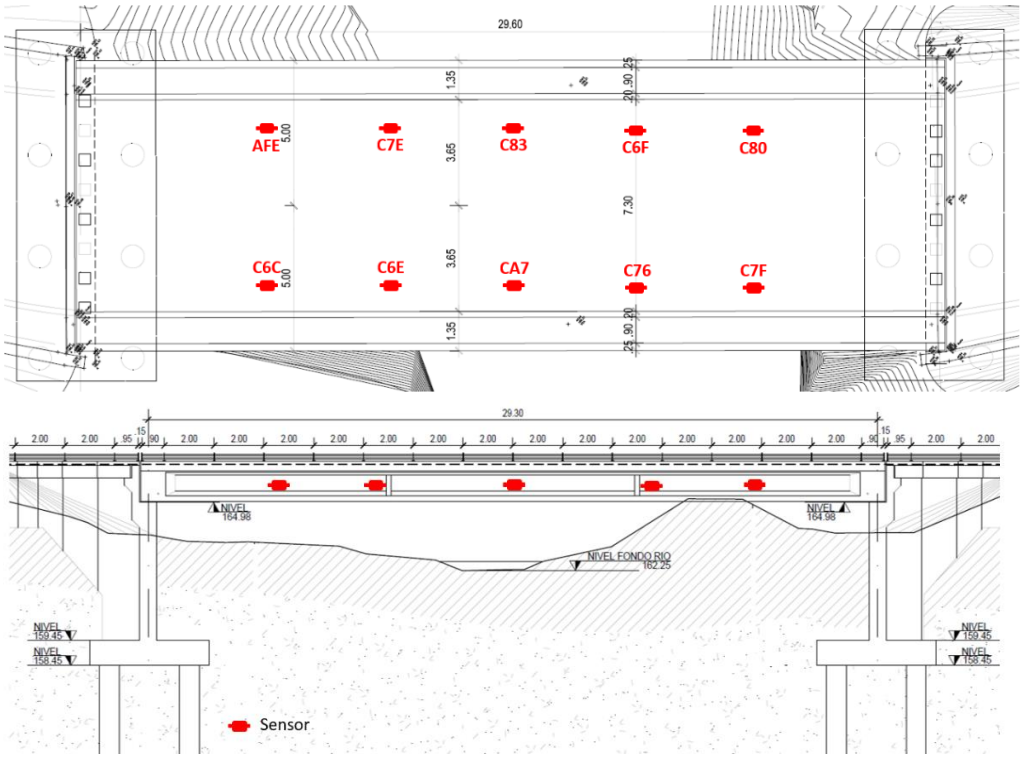

Fig. 7 SHM instrumentation and sensors locations

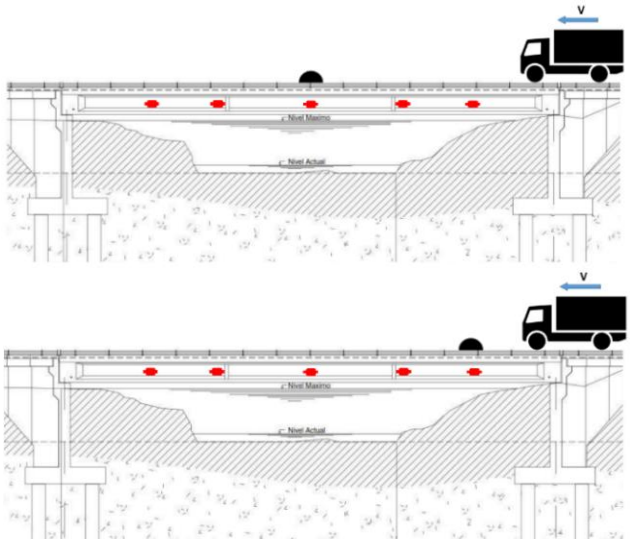

Fig. 8 Source locations; the excitation was induced by an impact from a truck moving through a bump

To provide an initial insight into the vibration characteristics of the structure the power spectral density (PSD) of a 5-minute record of ambient vibrations at locations CA7 and C6C (as per Fig. 7) are shown in Fig. 10. The PSD shows the power (related to the energy) of the frequency content of the vibration response. The PSD were estimated using the Barlett Method (Proakis and Manolakis, 1996). For ambient vibrations with a smooth and approximately constant PSD, the peaks of the vibration measurements PSD are close to the structure vibration frequencies, thus providing an initial estimate of the main vibration frequencies of the bridge.

Table 2 Estimated dynamic properties using the ERA and SSID methods

Mode	ERA		SSID	
	Frequency (Hz)	Damping (%)	Frequency (Hz)	Damping (%)
1	2.73	4.92	2.56	4.51
2	9.22	2.91	9.60	1.84
3	12.4	2.33	11.2	1.42
4	16.4	2.52	15.3	1.52

The estimation of the vibration frequencies and damping ratios can be improved by using state-of-the-art system identification methods (Ljung, 1998). The Eigen-Realization Algorithm (ERA) was used to estimate the dynamic properties for the free vibration case, while the covariance-based stochastic subspace identification (SSID) was used to estimate the dynamic properties for the ambient vibration case. The estimated properties are summarized in Table 2. As can be seen the estimated frequencies are close to the peaks of the output PSD shown in Fig. 10, with damping ratios in the range 1-5%. The dynamic properties estimates were used to develop a digital twin of the bridge. For this purpose the elastic modulus was adjusted so that the most important vibration frequencies (with higher response participation) match the identified frequencies. To adjust the elastic modulus the structure was first divided in several regions according to the girders locations, and the elastic modulus of each region was updated. The results showed that the spatial variability was considerably small due to the girders being precast under controlled fabrication conditions. For this reason it was decided to parameterize

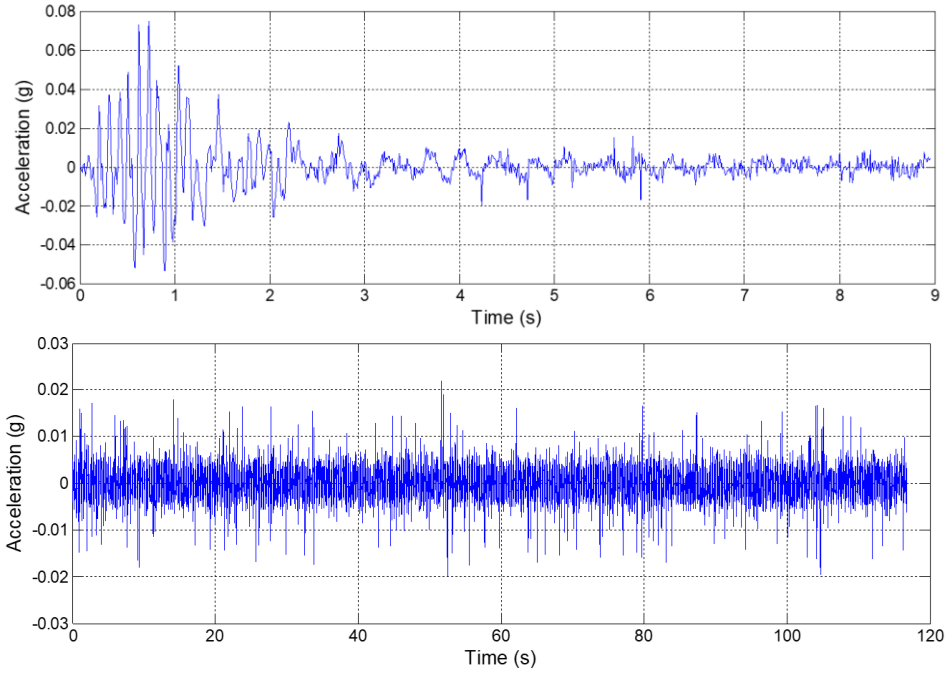

Fig. 9 Vibration measurements for free vibrations (top) and ambient vibrations (bottom)

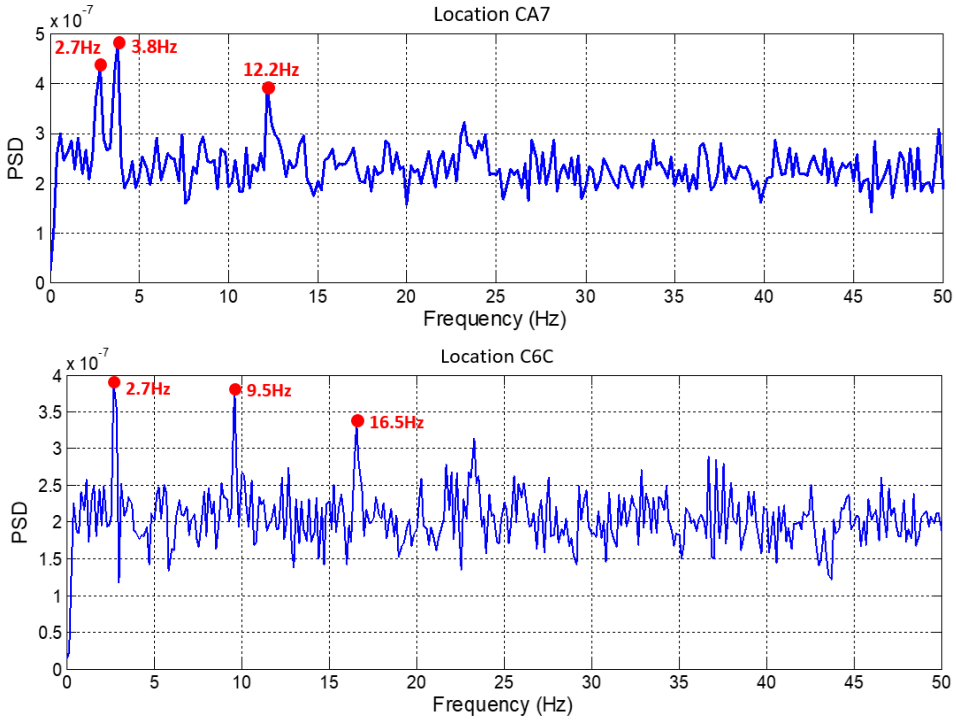

Fig. 10 Power spectral density for ambient vibrations at two locations

the flexural stiffness so that all the girders have the same elastic modulus.

The resulting frequency of the first mode of the updated model was 2.70Hz, which closely matches the identified frequency with ERA, while the frequency of the second mode was 9.24Hz which as seen in Fig. 10 is close to the second mode frequency; the vibration frequencies of the third and fourth modes were 11.3Hz and 15.5Hz respectively.

6. Development of fragility curves

A nonlinear time-history analysis was performed using the ground motion records previously discussed and the digital twin model of the bridge. The maximum unit deformations for the girders for each analysis (state S) are shown in Table 3 for various ground motion intensities defined by the PGA.

Table 3 Estimated concxrete maximum unit deformation for the bridge girders

PGA	S1	S2	S3	S4	S5	S6	S7	S8	S9	S10	S11
0.05g	0.0002	0.0001	0.0001	0.0002	0.0002	2E-04	0.0002	0.0002	0.0002	0.0002	0.0002
0.15g	0.0003	0.0003	0.0003	0.0006	0.0004	3E-04	0.0003	0.0003	0.0003	0.0004	0.0004
0.25g	0.0005	0.0004	0.0007	0.001	0.0006	5E-04	0.0005	0.0004	0.0005	0.0005	0.0006
0.35g	0.0007	0.0007	0.0015	0.0013	0.0007	7E-04	0.0008	0.0005	0.0006	0.0008	0.001
0.45g	0.0008	0.001	0.0022	0.002	0.0009	9E-04	0.0011	0.0008	0.0009	0.0012	0.0015
0.55g	0.0009	0.0014	0.0025	0.0031	0.0013	0.001	0.0012	0.0013	0.0013	0.0016	0.0019
0.65g	0.0012	0.0018	0.003	0.0041	0.002	0.001	0.0015	0.0016	0.002	0.0025	0.0027
0.75g	0.0015	0.0022	0.0035	0.0046	0.0027	0.002	0.002	0.002	0.0031	0.0035	0.0034
0.85g	0.0021	0.0026	0.0039	0.0053	0.0035	0.003	0.0027	0.0025	0.004	0.0044	0.0037
0.95g	0.003	0.0031	0.0043	0.0058	0.0038	0.004	0.0035	0.003	0.0044	0.0054	0.0042
1.05g	0.0039	0.0036	0.0048	0.0063	0.0041	0.004	0.004	0.0031	0.0048	0.0064	0.0047

Table 4 Events related to exceeding various damage limit states for different PGA

PGA	Number of Occurrences				Accumulated Occurrences			
	Minor	Moderate	Extensive	Complete	Minor	Moderate	Extensive	Complete
0.05	0	0	0	0	0	0	0	0
0.15	0	0	0	0	0	0	0	0
0.25	0	0	0	0	0	0	0	0
0.35	2	0	0	0	2	0	0	0
0.45	3	1	0	0	4	1	0	0
0.55	8	1	1	0	10	2	1	0
0.65	5	2	1	0	8	3	1	0
0.75	1	2	4	1	8	7	5	1
0.85	0	5	4	1	10	10	5	1
0.95	0	0	6	2	8	8	8	2
1.05	0	0	6	5	11	11	11	5

From the results shown in Table 3, the number of times that each damage state is attained or exceeded for each PGA can be determined; the results are shown in Table 4 for the different damage limit states.

To generate the fragility curves the values of the percentages obtained by each analysis (based on Table 4) were fitted to a lognormal probability distribution. The resulting model parameters for each limit state are presented in Table 5. The resulting fragility curves are shown in Fig. 11 for the different damage limit states considered in this study.

Based on the curves the probabilities of damage for an acceleration of 0.8g, which is the maximum expected acceleration (with 2% exceedance probability in 50 years) for the Moca region where the bridge is located, can be readily obtained. The probability of the structure presenting complete damage is approximately 9%, while the probability of the bridge presenting extensive damage is 62%. The probability of the structure experiencing moderate damage is 22%. From the resulting curves other damage limit states can be readily evaluated.

For an acceleration of 0.6g, which is the expected acceleration for the frequent earthquake (10% in 50 years), the probability of extensive damage is 7.5%, the probability of moderate damage is 30%, while the probability of mild damage is 60%. The probability that the structure does not suffer any type of damage is 2.5%. These results validate that this particular bridge is consistent with the design philosophy prescribed in the seismic code, since for the design earthquake the structure would experience extensive damage without collapse, while for the frequent earthquake the structure would suffer only minor damage.

In order to assess the effect of using a digital twin model the fragility curves are compared to the curves obtained based on the original computational model. The original computational model is based solely on the construction drawings for the bridge. The curves are presented in Fig. 12. As can be seen the original model significantly underestimates the probability of damage for the various limit states. For example, for a PGA of 0.8g the original model predicts a 50% probability of extensive damage, while the digital twin model predicts a 68% probability for the same limit state. Similarly for a PGA of 1.2g the original model predicts a 62% probability of complete damage, while the digital twin model predicts an 80% probability for the same limit state.

Table 5 Fragility curves model parameters fitted for different damage limit states and cumulative probability

	Minor		Moderate		Extensive		Complete	
PGA	μ	σ	μ	σ	μ	σ	μ	σ
	0.45	0.08	0.64	0.11	0.75	0.1	1.05	0.18
0	0.000		0.000		0.000		0.000	
0.05	0.000		0.000		0.000		0.000	
0.15	0.000		0.000		0.000		0.000	
0.25	0.006		0.000		0.000		0.000	
0.35	0.106		0.004		0.000		0.000	
0.45	0.500		0.042		0.001		0.000	
0.55	0.894		0.207		0.023		0.003	
0.65	0.994		0.536		0.159		0.013	
0.75	1.000		0.841		0.500		0.048	
0.85	1.000		0.972		0.841		0.133	
0.95	1.000		0.998		0.977		0.289	
1.05	1.000		1.000		0.999		0.500	
1.1	1.000		1.000		1.000		0.609	
1.2	1.000		1.000		1.000		0.803	
1.3	1.000		1.000		1.000		0.923	
1.4	1.000		1.000		1.000		0.975	
1.5	1.000		1.000		1.000		0.997	

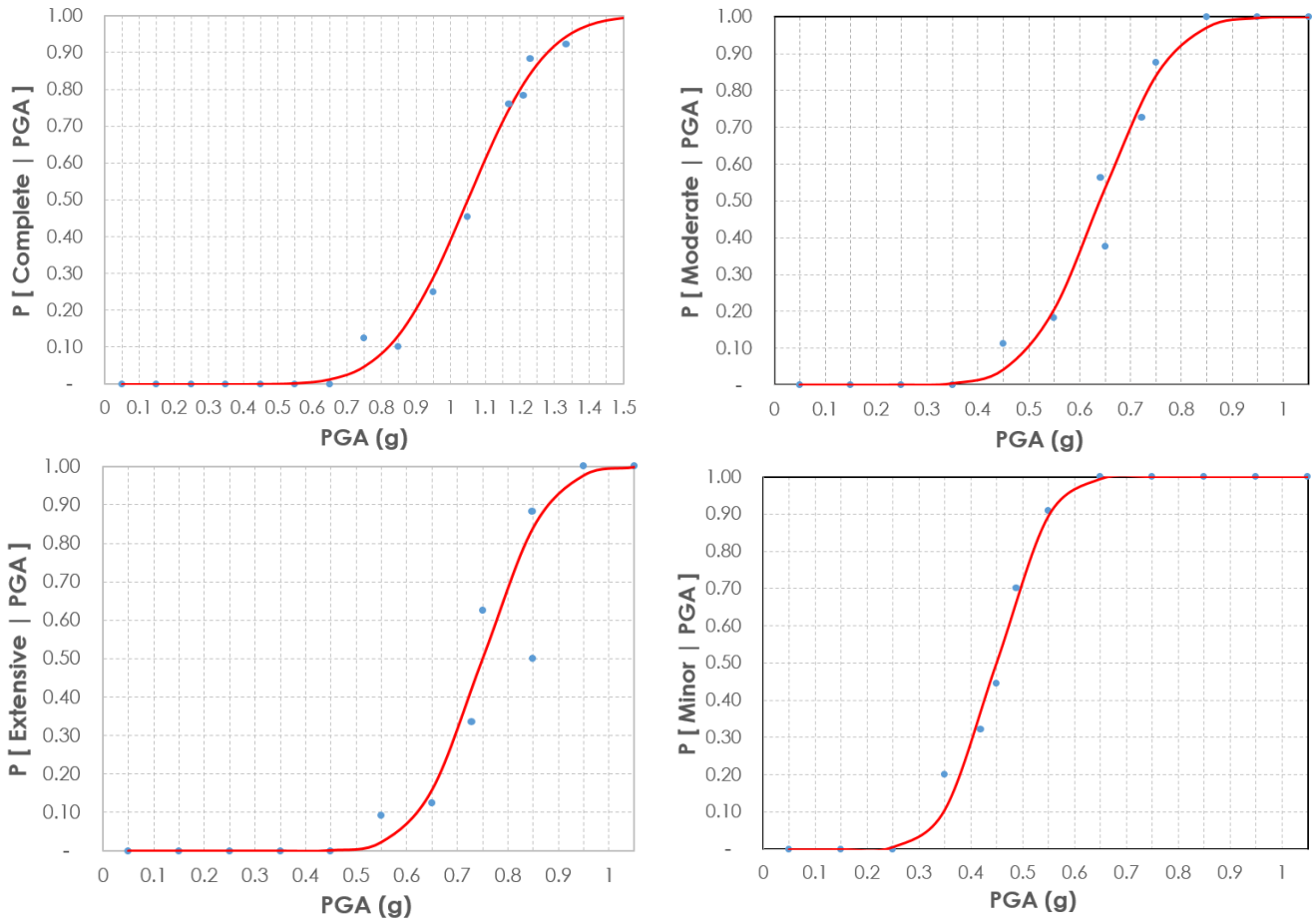

Fig. 11 Fragility curves for different damage limit states

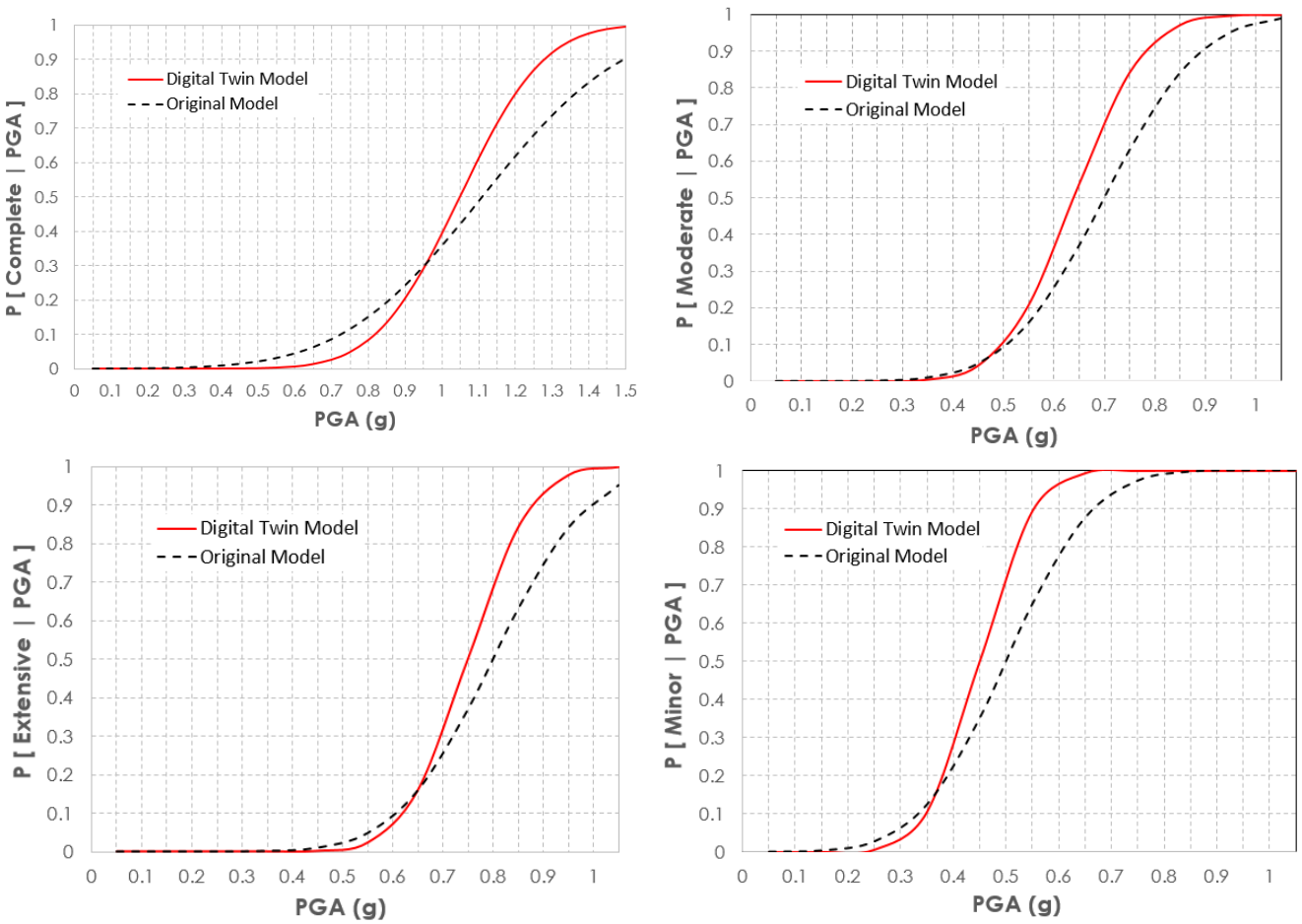

Fig. 12 Fragility curves based on the digital twin model and the original computational model

The fragility curves developed in this study can be employed to estimate the performance of similar bridges when subjected to earthquake induced ground motions. The curves provide an additional tool for the seismic vulnerability assessment of bridges, as well as for disaster mitigation decision-making strategies.

7. Conclusions

In this paper a set of fragility curves are developed for a precast concrete bridge in the Dominican Republic (DR). The bridge is located in a region of high seismic hazard providing the only access to several communities after the potential occurrence of a major earthquake or other severe natural events. To improve the state of knowledge of the state of structural integrity of the bridge a structural health monitoring (SHM) system was installed and used to extract information related to the vibration characteristics of the structure. The parameters estimated from the SHM data were combined with a computational structural model to develop a digital twin which was used to formulate a set of fragility curves for different damage limit states.

The fragility curves developed provide a quantitative measure of expected damage (in probabilistic terms) to estimate the probability that the structure will exceed various structural damage limit states as a function of an earthquake intensity measure, providing a quantitative measure of structural performance. The digital twin was developed by combining a nonlinear finite element model with the information extracted from the SHM system installed on the bridge, reducing modeling uncertainty and significantly improving the predicting capability of the model. The digital twin was used to perform a nonlinear time-history analysis with selected ground motions that are consistent with the seismic fault and site characteristics.

The fragility curves generated show that for the maximum expected acceleration (with a 2% exceedance probability in 50 years) the structure has a 62% probability of undergoing extensive damage. Similarly, for a ground acceleration with 10% exceedance probability in 50 years the bridge has a 60% probability of experiencing minor damage. When evaluating the structure for an acceleration of 0.6g, which is the expected maximum acceleration for the frequent earthquake (10% exceedance probability in 50 years), the probability of extensive damage was 7.5%, the probability of moderate damage was 30% and the probability of minor damage was 60%; the probability that the structure does not suffer any type of damage was 2.5%. The study also compares the fragility curves obtained from the digital twin and the original computational models; it is shown that the fragility curves are sensitive to the model

employed, and thus a digital twin model provides an estimate that is consistent with the actual structure characteristics. This study provides the first fragility curves for civil infrastructure in the DR, and the methodology can be similarly applied to other types of structures.

Acknowledgments

This work was partially supported by the Ministry of Higher Education, Sciences and Technology of the Dominican Republic (MESCYT). The support is gratefully acknowledged.

References

AASHTO (2012), *LRFD Bridge Design Specifications*, American Association of State Highway and Transportation Officials, Washington D.C., USA.

Avşar, Ö., Yakut, A. and Caner, A. (2011), "Analytical fragility curves for ordinary highway bridges in Turkey", *Earthq. Spectra*, **27**(4), 971-996. https://doi.org/10.1193/1.3651349.

Baker, J. W. (2015), "Efficient analytical fragility function fitting using dynamic structural analysis", *Earthq. Spectra*, **31**, 579-599. https://doi.org/10.1193/021113EQS025M.

Bakhshinezhad, S. and Mohebbi, M. (2019), "Multiple failure criteria-based fragility curves for structures equipped with SATMDs", *Earthq. Struct.*, **17**(5), 463–475. https://doi.org/10.12989/EAS.2019.17.5.463.

Batista, L. (2017), Por lluvias 42 puentes colapsan en la región sur, informa Obras Públicas; Diario Libre, Dominican Republic. https://www.diariolibre.com/actualidad/por-lluvias-42-puentes-colapsan-en-la-region-sur-informa-obras-publicas-KG6976963

Calais, E., Béthoux, N. and de Lépinay, B.M. (1992), "From transcurrent faulting to frontal subduction: A seismotectonic study of the northern Caribbean plate boundary from Cuba to Puerto Rico", *Tectonics*, **11**, 114–123. https://doi.org/10.1029/91TC02364.

Calais, E., Mazabraud, Y., Mercier de Lépinay, B., Mann, P., Mattioli, G. and Jansma, P. (2002), "Strain partitioning and fault slip rates in the northeastern Caribbean from GPS measurements", *Geophys. Res. Lett.*, **29**(18), 3-11. https://doi.org/10.1029/2002GL015397.

Calvi, G.M. (1999), "A displacement-based approach for vulnerability evaluation of classes of buildings", *J. Earthq. Eng.*, **3**(3), 411-438. https://doi.org/10.1142/S136324699900017X.

CSiBridge (2020), *CSiBridge*, *Bridge Analysis*, *Design and Rating*; Computers and Structures, Inc., USA. https://www.csiamerica.com

De Risi, R., DiSarno, L. and Paolacci, F. (2017), "Probabilistic seismic performance assessment of an existing RC bridge with portal-frame piers designed for gravity loads only", *Eng. Struct.*, **145**(15), 348-367. https://doi.org/10.1016/j.engstruct.2017.04.053.

DesRoches, R., Comerio, M., Eberhard, M., Mooney, W. and Rix, G. (2011), "Overview of the 2010 Haiti earthquake", *Earthq. Spectra*, **27**(S1), 1–21. https://doi.org/10.1193/1.3630129.

Elnashai, A. and Di Sarno, L. (2008), *Fundamentals of Earthquake Engineering*, Wiley and Sons, UK.

Erazo, K. (2019), "Probabilistic seismic hazard analysis and design earthquake for Santiago, Dominican Republic", *Ciencia, Ingenierías Y Aplicaciones*, **2**(1), 67-84. https://doi.org/10.22206/cyap.2019.v2i1.pp67-84.

Erazo, K. (2020), "Análisis probabilístico de peligro sísmico y terremoto de diseño para Santiago-República Dominicana", *Ciencia, Ingenierías Y Aplicaciones*, **3**(1), 7-30. https://doi.org/10.22206/cyap.2020.v3i1.pp7-30.

Erazo, K., Moaveni, B. and Nagarajaiah, S. (2019a), "Bayesian seismic strong-motion response and damage estimation with application to a full-scale seven story shear wall structure", *Eng. Struct.*, **186**, 146-160. https://doi.org/10.1016/j.engstruct.2019.02.017.

Erazo, K., Sen, D., Nagarajaiah, S. and Sun, L. (2019b), "Vibration-based structural health monitoring under changing environmental conditions using Kalman filtering", *Mech. Syst. Signal Process.*, **117**, 1-15. https://doi.org/10.1016/j.ymssp.2018.07.041.

Feng, R., Wang, X., Yuan, W. and Yu, J. (2018), "Impact of seismic excitation direction on the fragility analysis of horizontally curved concrete bridges", *Bullet. Earthq. Eng.*, **16**(10), 4705-4733. https://link.springer.com/article/10.1007/s10518-018-0400-2.

Frankel A, Harmsen S, Mueller C, Calais E. and Haase J (2011), "Documentation for initial seismic hazard maps for Haiti", *Earthq. Spectra*, **27**(S1), S23–S41. https://doi.org/10.3133/ofr20101067.

GFDR (2007), ThinkHazard; World Bank Group, Washington D.C., USA. http://thinkhazard.org.

Gómez, C. and Soria, I. (2013), "Curvas de fragilidad para tres puentes carreteros típicos de concreto", *Concreto Y Cemento. Investigación y Desarrollo*, **4**(2), 26-42.

Iervolino, I., Galasso, C. and Cosenza, E. (2010), "REXEL: Computer aided record selection for code-based seismic structural analysis", *Bullet. Earthq. Eng.*, **8**, 339-362. https://doi.org/10.1007/s10518-009-9146-1.

INFORM (2019), *Index for Risk Management*, Disaster Risk Management Knowledge Centre, European Commission, Brussels, Belgium.

Ljung, L. (1998), *System Identification*, Birkhäuser, MA, Boston, USA.

Karimzadeh, S., Kadas, K., Askan, A., Erberik, M. A. and Yakut, A. (2020), "Derivation of analytical fragility curves using SDOF models of masonry structures in Erzincan (Turkey)", *Earthq. Struct.*, **18**(2), 249-261. https://doi.org/10.12989/eas.2020.18.2.249.

Kehila, F., Kibboua, A., Bechtoula, H. and Remki, M. (2018), "Seismic performance assessment of R.C. bridge piers designed with the Algerian seismic bridges regulation", *Earthq. Struct.*, **15**(6), 701-713. https://doi.org/10.12989/EAS.2018.15.6.701.

Mann, P., Taylor, F.W., Lawrence, R. and Ku, Teh-Lung (1994), "Actively evolving microplate formation by oblique collision and sideways motion along strike-slip faults: An example from the northeastern Caribbean plate margin", *Tectonophysics*, **246**, 1-69. https://doi.org/10.1016/0040-1951(94)00268-E.

Mangalathu, S., Hwang, S.H., Choi, E. and Jeon, J.S. (2019), "Rapid seismic damage evaluation of bridge portfolios using machine learning techniques", *Eng. Struct.*, **201**, 109785. https://doi.org/10.1016/j.engstruct.2019.109785.

Mangalathu, S. and Jeon, J.S. (2019), "Stripe-based fragility analysis of multispan concrete bridge classes using machine learning techniques", *Earthq. Eng. Struct. Dynam.*, **48**(11), 1238-1255. https://doi.org/10.1002/eqe.3183.

Martin, J., Alipour, A. and Sarkar, P. (2019), "Fragility surfaces for multi-hazard analysis of suspension bridges under earthquakes and microbursts", *Eng. Struct.*, **197**, 109169. https://doi.org/10.1016/j.engstruct.2019.05.011.

Mieses, L.A., López, R.R. and Saffar, A. (2007), "Development of fragility curves for medium rise reinforced concrete shear wall residential buildings in Puerto Rico", *Mecánica Computacional*, **31**, 2712-2727.

Ministerio de Obras Públicas y Comunicaciones (2011), "Reglamento para el análisis y diseño sísmico de estructuras, R-001", Ph.D. Dissertation; Pedro Henriquez Ureña National University, Santo Domingo.

Moschonas, I.F., Kappos, A. J., Panetsos, P., Papadopoulos, V., Makarios, T. and Thanopoulos, P. (2009), "Seismic fragility curves for greek bidges: Methodology and case studies", *Bullet. Earthq. Eng.*, **7**, 439-468. https://doi.org/10.1007/s10518-008-9077-2.

Nagarajaiah, S. and Erazo, K. (2016), "Structural monitoring and identification of civil infrastructure in the United States", *Struct. Monitor. Maintenance*, **3**(1), 51. https://doi.org/10.12989/smm.2016.3.1.051.

Naderpour, H. and Vakili, K. (2019), "Safety assessment of dual shear wall-frame structures subject to Mainshock-Aftershock sequence in terms of fragility and vulnerability curves", *Earthq. Struct.*, **16**(4), 425-436. https://doi.org/10.12989/EAS.2019.16.4.425.

Neris, K., Domínguez, J., Pérez, J., Rodríguez, B. and Cano, E. (2010), "Control de la edificación como medida de reducción de riesgo al desastre causado por sismos en la República Dominicana", *1er Congreso Iberoamericano de Ingeniería de Proyectos*, Zaragoza, Spain, May.

Nielson, B.G. (2005), "Analytical Fragility Curves for Highway Bridges in Moderate Seismic Zones", Ph.D. Dissertation, Georgia Institute of Technology, Atlanta.

Nielson, B. and DesRoches, R. (2007), "Analytical seismic fragility curves for typical bridges in the central and southeastern united states", *Earthq. Spectra*, **23**(3), 615-633. https://doi.org/10.1193/1.2756815.

Padgett, J. and DesRoches, R. (2008), "Methodology for the development of analytical fragility curves for retrofitted bridges", *Earthq. Eng. Struct. Dynam.*, **37**, 1157–1174. https://doi.org/10.1002/eqe.2774.

Proakis, J. and Manolakis, D. (1996), *Digital Signal Processing: Principles, Algorithms and Applications*, Prentice Hall, NJ, USA.

Razzaghi, M. S., Safarkhanlou, M., Mosleh, A. and Hosseini, P. (2018), "Fragility assessment of RC bridges using numerical analysis and artificial neural networks", *Earthq. Struct.*, **15**(4), 431–441. https://doi.org/10.12989/EAS.2018.15.4.431.

Rodríguez, V. and López, Y. (2007), Puentes y caminos de frágil resistencia; Listin Diario, Dominican Republic. https://listindiario.com/ld-lecturas-de-domingo/2007/11/12/36312/puentes-y-caminos-de-fragil-resistencia

Rossetto, T and Elnashai, A. (2005), "A new analytical procedure for the derivation of displacement-based vulnerability curves for populations of RC structures", *Eng. Struct.*, **27**(3), 397-409. https://doi.org/ 10.1016/j.engstruct.2004.11.002.

Shinozuka, M., Qing Feng, M., Lee, J. and Naganuma, T. (2000), "Statistical analysis of fragility curves", *J. Eng. Mech.*, **126**(12), https://doi.org/10.1061/(ASCE)0733-9399(2000)126:12(1224).

Surana, M. (2020), "Seismic fragility curves using pulse-like and spectrally equivalent ground-motion Records", *Earthq. Struct.*, **19**(2), 79-90. https://doi.org/10.12989/EAS.2020.19.2.079.

Tavares, D., Padgett, J. and Paultre, P. (2012), "Fragility curves of typical as-built highway bridges in eastern Canada", *Eng. Struct.*, **40**, 107-118. https://doi.org/10.1016/j.engstruct.2012.02.019.

Wilches, J., Santa María, H., Riddel, R. and Arrate, C. (2019), "Fragility curves for a typical Chilean higway bridge", *Bridge Engineering Institute Conference* (BEI-2019), Honolulu, Hawaii, July.

Wu, D., Tesfamariam, S., Stiemer, S.F. and Qin, D. (2012), "Seismic fragility assessment of RC frame structure designed according to modern Chinese code for seismic design of buildings", *Earth. Eng. Eng. Vib.*, **11**(3), 331-342. https://doi.org/10.1007/s11803-012-0125-1.

Yamaguchi, N. and Yamazaki, F. (2000), "Fragility curves for buildings in Japan based damaged surveys after the 1995 Kobe Earthquake", *12th World Conference of Earthquake Engineering*, Auckland, January.

Yazdabad, M., Behnamfar, F. and Samani, A.K. (2018), "Seismic behavioral fragility curves of concrete cylindrical water tanks for sloshing, cracking and wall bending", *Earthq. Struct.*, **14**(2), 95–102. https://doi.org/10.12989/EAS.2018.14.2.095.

Yon, B. (2020), "Seismic vulnerability assessment of RC buildings according to the 2007 and 2018 Turkish seismic codes", *Earthq. Struct.*, **18**(6), 709-718. https://doi.org/10.12989/EAS.2020.18.6.709.

Zhang, J.H. and Hu, S.D. (2005), "State of the Art of Bridge Seismic Vulnerability Analysis Research", *Struct. Eng*, **21**(5), 76-80. https://doi.org/10.3969/j.issn.1005-0159.2005.05.017.

Zhao, Y., Hu, H., Bai, L., Tang, M., Chen, H. and Su, D. (2021), "Fragility analyses of bridge structures using the logarithmic piecewise function-based probabilistic seismic demand model", *Sustainability*, **13**(14), 7814. https://doi.org/10.3390/su13147814.

DL